Resting-State Functional Brain Connectivity: Lessons from Functional Near-Infrared Spectroscopy

Haijing Niu and Yong He

Neuroscientist 2014 20: 173 originally published online 10 September 2013
DOI: 10.1177/1073858413502707

The Neuroscientist
2014, Vol. 20(2) 173–188

DOI: 10.1177/1073858413502707
nro.sagepub.com
SAGE

Resting-State Functional Brain Connectivity: Lessons from Functional Near-Infrared Spectroscopy

Haijing Niu[1] and Yong He[1]

Abstract

Resting-state functional near-infrared spectroscopy (R-fNIRS) is an active area of interest and is currently attracting considerable attention as a new imaging tool for the study of resting-state brain function. Using variations in hemodynamic concentration signals, R-fNIRS measures the brain's low-frequency spontaneous neural activity, combining the advantages of portability, low-cost, high temporal sampling rate and less physical burden to participants. The temporal synchronization of spontaneous neuronal activity in anatomically separated regions is referred to as resting-state functional connectivity (RSFC). In the past several years, an increasing body of R-fNIRS RSFC studies has led to many important findings about functional integration among local or whole-brain regions by measuring inter-regional temporal synchronization. Here, we summarize recent advances made in the R-fNIRS RSFC methodologies, from the detection of RSFC (e.g., seed-based correlation analysis, independent component analysis, whole-brain correlation analysis, and graph-theoretical topological analysis), to the assessment of RSFC performance (e.g., reliability, repeatability, and validity), to the application of RSFC in studying normal development and brain disorders. The literature reviewed here suggests that RSFC analyses based on R-fNIRS data are valid and reliable for the study of brain function in healthy and diseased populations, thus providing a promising imaging tool for cognitive science and clinics.

Keywords

connectome, connectomics, small-world, graph theory, network, functional connectivity, fNIRS

Introduction

The human brain is a complex and dynamic system and is often represented as a structurally or functionally interconnected network that works to ensure both continuous processing and efficient information flow between interconnected units (He and Evans 2010; Sporns 2013). Examining neural connectivity patterns can provide valuable insight into how the human brain operates (Bassett and Gazzaniga 2011). Recent research has shown that modern neuroimaging and neurophysiological techniques (e.g., fMRI, electroencephalography/magnetoencephalography [EEG/MEG], and functional near-infrared spectroscopy [fNIRS]) are important tools for exploring functional integration among brain regions during different states, including the resting and task states in normal people and patients with neurological and psychiatric disorders (Bassett and Bullmore 2009; He and Evans 2010; Sporns 2013; Xia and He 2011; Yu and others 2012).

Functional near-infrared spectroscopy is a promising technology with a high temporal sampling rate, long period of continuous data acquisition, and low physical burden on the participants. As an emerging neuroimaging tool, fNIRS has been successfully used to localize brain activation during cognitive engagement (Gervain and others 2008; Nakano and others 2009; Niu and others 2010; Sugiura and others 2011; Taga and others 2003; Zeff and others 2007) and to identify functional connectivity during resting-state brain activity (Homae and others 2010; Lu and others 2010; Mesquita and others 2010; Niu and others 2012; Sasai and others 2011; White and others 2012; White and others 2009; H. Zhang and others 2010; Y.-J. Zhang and others 2010). To date, several typical approaches for the analysis of resting-state functional connectivity (RSFC) using other imaging modalities

[1]State Key Laboratory of Cognitive Neuroscience and Learning & IDG/McGovern Institute for Brain Research, Beijing Normal University, Beijing, China

Corresponding Author:
Yong He, State Key Laboratory of Cognitive Neuroscience and Learning & IDG/McGovern Institute for Brain Research, Beijing Normal University, Beijing 100875, China.
Email: yong.he@bnu.edu.cn

(e.g., fMRI and EEG/MEG) have also been applied to resting-state fNIRS (R-fNIRS) to characterize the local- or whole-brain functional connectivity. These approaches primarily include seed-based correlation analysis, independent component analysis (ICA), whole-brain correlation analysis, and graph-theoretical topological analysis (see the Resting-State Functional Connectivity Section under "Basic Concepts"). Here, we conducted a literature search on PubMed (www.ncbi.nlm.nih.gov/pubmed) using key words such as ((NIRS [All Fields] OR fNIRS [All Fields]) OR optical [All Fields]) AND ((resting-state [All Fields] AND functional connectivity [All Fields]) OR (resting-state [All Fields] AND functional networks [All Fields])), and 15 publications were identified in the human brain research field (Table 1).

In this review, we summarize these recent advances made in the study of RSFC derived from R-fNIRS data, focusing mainly on areas of ongoing research and application. This study will hopefully generate more excitement about the emerging R-fNIRS RSFC field. This article is organized into three main sections. First, we introduce several basic principles and concepts regarding fNIRS and brain connectivity. Then, we review a series of R-fNIRS studies from three perspectives: RSFC detection methods (e.g., seed-based correlation analysis, ICA, whole-brain correlation analysis, and graph-theoretical topological analysis), RSFC performance assessment (e.g., reliability, reproducibility, and validity) and its relevant applications. Finally, we highlight future directions and challenging issues within the R-fNIRS RSFC research field.

Basic Concepts

R-fNIRS Imaging Systems

Multiple optical instruments have been applied to R-fNIRS studies for the measurement of the hemodynamic response in human brain tissue, which include the CW5/CW6 system (TechEn, Milford, MA; Mesquita and others 2010; Niu and others 2011; Niu and others 2012, 2013), the DYNOT system (NIRx Medical Technologies, New York, NY) (Niu and others 2011), a customized high-density diffuse optical tomography (DOT) system (White and others 2009; White and others 2012), and the ETG100/4000/ETG7000 systems (Hitachi Medical Co., Tokyo, Japan) (Duan and others 2012; Homae and others 2010; Lu and others 2010; Sasai and others 2012; Zhang and others 2011; H Zhang and others 2010; Y-J Zhang and others 2010). All of these are continuous wave (CW) instruments and are currently considered to be more readily commercially available than other imaging-domain systems, such as those based on frequency or time domains. In CW systems, light sources emit light continuously, either at a constant intensity or are modulated at a low (a few kilohertz) frequency, and the absorption changes in tissue are determined by measuring the attenuation of the incident light.

General Principles of R-fNIRS Detection

Human brain tissue is a turbid media in which near-infrared (NIR) light (650-1000 nm) is diffused by tissue cells and is absorbed mainly by oxygenated hemoglobin (HbO_2) and deoxygenated hemoglobin (HbR) (Ferrari and Quaresima 2012; Jobsis 1977; Wray and others 1988). Given that the two chromophores have distinct absorption spectra in the NIR range, neural activity–based changes in HbO_2 and HbR concentrations in the cerebral cortex can be quantified using two or more wavelengths (Boas and others 2004; Jobsis 1977; Zhang and others 2012). During image collection, sources are fixed into a custom holder and are then placed adjacent to the scalp, allowing the NIR light to penetrate the scalp, skull, and cerebrospinal fluid to reach the cortical layers of the brain (Jobsis 1977). The reflected light from the cortical tissue is then received by detectors that are positioned a few centimeters away from the sources. Typically, a source–detector pair with a separation of approximately 3 cm is considered to be able to effectively record cortical brain tissue activation (Niu and others 2010; Tian and others 2011).

The concentration calculation of HbO_2 and HbR in the continuous wave systems is mainly based on the Beer–Lambert law (Cope and Delpy 1988). When light of a certain wavelength λ_1 passes through a nonscattering homogeneous medium, the incremental optical density (ΔOD) from the reference is expressed as

$$\Delta OD = -\log I / I_0 = \varepsilon \cdot \Delta C \cdot L \quad (1)$$

where I and I_0 are the intensities of the detected and illuminated light, respectively, ε is the molar absorption coefficient, C is concentration, and L is the length that light travels through the medium (optical pathlength) (Arridge and others 1992; Delpy and others 1988). For a light-scattering system such as brain tissue, the change of optical density is modified according to the Beer–Lambert law (Cope and Delpy 1988; Delpy and others 1988):

$$\Delta OD_{\lambda_1} = (\varepsilon^{\lambda_1}_{HbO_2} \cdot \Delta C_{HbO_2} + \varepsilon^{\lambda_1}_{HbR} \cdot \Delta C_{HbR}) \cdot L^{\lambda_1} + S_{\lambda_1} \quad (2)$$

where $S_{\lambda 1}$ refers to the optical attenuation mainly due to scattering, ε is the molar absorption coefficient of HbO_2 or HbR, ΔC represents the concentration changes of HbO_2 or HbR (unit: μmol/L or μM). To minimize the effect of $S_{\lambda 1}$, a dual-wavelength method is often used (Cope and Delpy 1988; Delpy and others 1988). For λ_2, the optical density is written as

Table 1. Overview of R-fNIRS RSFC Studies.

Study	Subjects	Instrument	Sources/Detectors	Wavelengths (nm)	Brain Regions	Analytical Methods
White and others (2009)	5 adults	Custom-built DOT	24S/28D 24S/18D	750/850	Sensorimotor, visual cortex	Seed-based correlation analysis
Lu and others (2010)	29 adults	ETG-4000	17S/16D	695/830	Sensorimotor, auditory	Seed-based correlation analysis
H. Zhang and others (2010)[a]	21, 19 adults	ETG-4000	17S/16D	695/830	Sensorimotor, visual	ICA
Homae and others (2010)	52 infants	ETG-7000	30S/30D	785/830	Whole-head	Whole-brain correlation analysis
Y-J Zhang and others (2010)	30 adults	ETG-4000	8S/7D	695/830	Frontal, temporal	Seed-based correlation analysis
Mesquita and others (2010)	11 adults	CW5	16S/32D	690/830	Whole-head	Seed-based correlation analysis
H. Zhang and others (2010)	16 adults	ETG-4000	17S/16D	695/830	Sensorimotor	ICA
Sasai and others (2011)	21 adults	ETG-100	10S/8D	695/830	Whole-head	Whole-brain correlation analysis
Niu and others (2011)[b]	8, 9 adults	CW5, DYNOT	10S/16D, 32S/32D	695/830, 760/830	Sensorimotor	Seed-based correlation analysis
Zhang and others (2011)	21 adults	ETG-4000	17S/16D	695/830	Sensorimotor	Seed-based correlation analysis
White and others (2012)	8 infants	Custom-built DOT	18S/16D	750/850	Visual	Seed-based correlation analysis, ICA
Duan and others (2012)	21 adults	ETG-4000	8S/8D	695/830	Sensorimotor	Seed-based correlation analysis, graph-theory analysis
Sasai and others (2012)	28 adults	ETG-4000	8S/8D	695/830	Whole-head	Seed-based correlation analysis
Niu and others (2012)	15 adults	CW6	12S/24D	690/830	Whole-head	Graph-theory analysis
Zhang and others (2012)	21 adults	ETG-4000	17S/16D	695/830	Sensorimotor	Whole-brain correlation analysis
Niu and others (2013)	18 adults	CW6	12S/24D	690/830	Whole-head	Graph-theory analysis

R-fNIRS = resting-state functional near-infrared spectroscopy; RSFC = resting-state functional connectivity; DOT = diffuse optical tomography; ICA = independent component analysis.
[a]For this study, 21 subjects were scanned at the sensorimotor areas and 19 at the visual regions.
[b]For this study, 8 subjects were scanned using the CW5 system and 9 using the DYNOT system.

$$\Delta OD_{\lambda_2} = (\varepsilon_{HbO_2}^{\lambda_2} \cdot \Delta C_{HbO_2} + \varepsilon_{HbR}^{\lambda_2} \cdot \Delta C_{HbR}) \cdot L^{\lambda_2} + S_{\lambda_2} \quad (3)$$

Therefore, by measuring the changes in the optical densities at two wavelengths, the concentration changes of HbO_2 and HbR in tissue can be calculated as

$$\Delta C_{HbR} = \frac{\varepsilon_{HbO_2}^{\lambda_1} \cdot (\Delta OD_{\lambda_2} / L^{\lambda_2}) + \varepsilon_{HbO_2}^{\lambda_2} \cdot (\Delta OD_{\lambda_1} / L^{\lambda_1})}{\varepsilon_{HbO_2}^{\lambda_1} \cdot \varepsilon_{HbR}^{\lambda_2} - \varepsilon_{HbO_2}^{\lambda_2} \cdot \varepsilon_{HbR}^{\lambda_1}} \quad (4)$$

$$\Delta C_{HbO_2} = \frac{\varepsilon_{HbR}^{\lambda_1} \cdot (\Delta OD_{\lambda_2} / L^{\lambda_2}) + \varepsilon_{HbR}^{\lambda_2} \cdot (\Delta OD_{\lambda_1} / L^{\lambda_1})}{\varepsilon_{HbR}^{\lambda_1} \cdot \varepsilon_{HbO_2}^{\lambda_2} - \varepsilon_{HbR}^{\lambda_2} \cdot \varepsilon_{HbO_2}^{\lambda_1}} \quad (5)$$

The summation of the changes in HbO_2 and HbR provide variations in the total hemoglobin (HbT), which reflects the variable blood flow within the tissue. Of note, the optical pathlength (L) in the tissue is longer than the physical one (the distance between the sources and detectors) due to the scattering effect, such that (Arridge and others 1992; Delpy and others 1988)

$$L = DPF \cdot d \quad (6)$$

where d is the distance between the light source and the detector and DPF is the differential pathlength factor that indicates the lengthening of the average optical pathlength due to light scattering in tissue. DPF has been measured in participants with a range of ages (Strangman and others 2003).

Resting-State Functional Connectivity

The resting state is a natural condition in which there is neither overt perceptual input nor behavioral output. Because this state is convenient to achieve, comparable across different studies, and reflects spontaneous or intrinsic brain activity, the resting state is a vital experimental

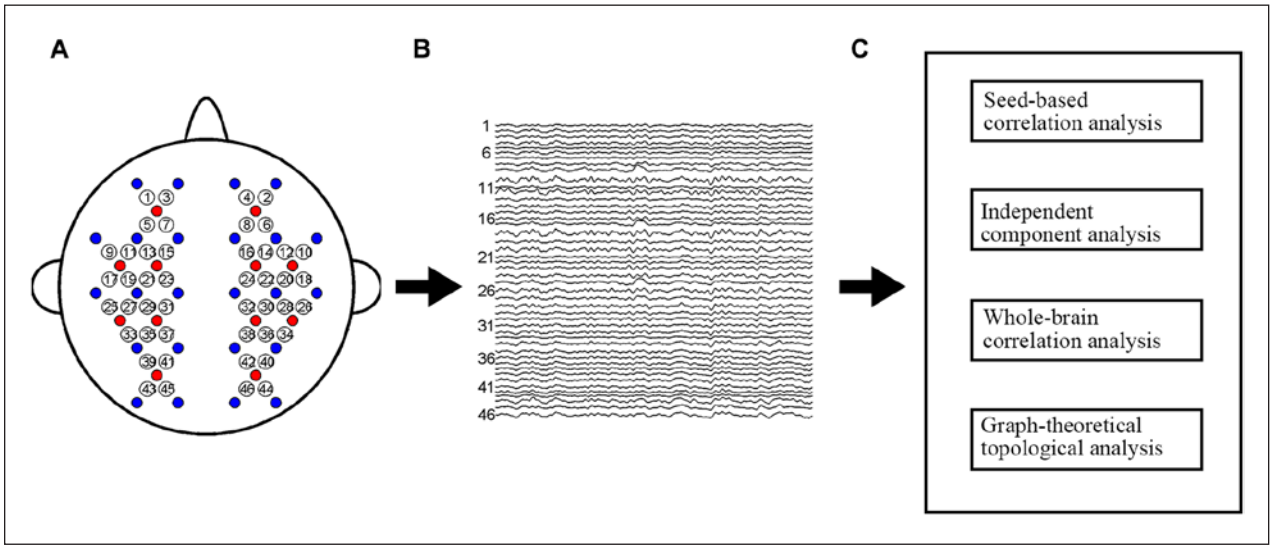

Figure 1. Diagram for R-fNIRS RSFC analysis. The charts represent the (A) R-fNIRS data collection, in which sources (red) and detectors (blue) were symmetrically placed on the left and right hemispheres and the adjacent source and detector constitute one measurement channel (46 channels for this probe arrangement), (B) calculation of hemoglobin concentration signal at each channel, and (C) RSFC analysis approaches based on the concentration signals. R-fNIRS = resting-state functional near-infrared spectroscopy; RSFC = resting-state functional connectivity.

paradigm for the study of brain function (Fox and Raichle 2007; Zhang and Raichle 2010). Functional connectivity derived from resting-state brain activity (i.e., RSFC) measures the temporal synchronization of spontaneous neuronal activation patterns of anatomically separated brain regions (Fox and Raichle 2007). In the past several years, an increasing body of research from different modalities has begun to explore RSFC between brain regions, and significant progress has been made. While the study of RSFC is an emerging topic in the R-fNIRS field, it is attracting increasing attention. Currently, four different types of R-fNIRS RSFC approaches have been used (Fig. 1): (1) the seed-based correlation analysis, which computes temporal correlations between a predefined channel of interest and other channels; (2) the independent component analysis or ICA, which uses the whole data set (i.e., all channels) to divide the brain into several statistically independent functional systems; (3) whole-brain correlation analysis, which examines the temporal correlation of time series between any two measurement channels in the whole brain; and (4) graph-theoretical topological analysis, which describes the topological organization patterns of brain networks.

Resting-State Functional Connectivity Studies Using R-fNIRS

R-fNIRS RSFC studies have been attracting increasing attention. To date, interesting progress has been made in three categories: RSFC detection methodologies, RSFC performance assessment, and the relevant applications of RSFC (Table 1).

Methodologies of RSFC Detection

Seed-based correlation analysis. The basic idea behind seed-based RSFC detection is the estimation of the strength of pairwise relationships between the seed regions (usually defined in terms of anatomical location or stimulus-induced activation foci) and all other regions in the brain. Using this method, several R-fNIRS studies have identified intrinsic functional connectivity in different brain systems (Fig. 2), such as the sensorimotor (Lu and others 2010; White and others 2009; White and others 2012), visual (White and others 2009), auditory (Lu and others 2010), and language systems (Y-J Zhang and others 2010). For example, White and others (2009) investigated RSFC in bilateral motor and visual regions of five participants. They found that the functional connectivity maps in each subject identified regions of the motor and visual cortices that highly resembled well-known functional networks that had been measured by fMRI. The functional connectivity maps were reproducible across sessions and subjects, demonstrating the feasibility and usefulness of the R-fNIRS technique for resting-state brain network detection. Using the seed-correlation approach, Lu and others (2010) examined the RSFC in the auditory systems of a group of 29 subjects. Unlike in White and others' work, Lu and others analyzed the group-level RSFC and found a high degree of functional connectivity in the bilateral auditory systems. This connectivity was

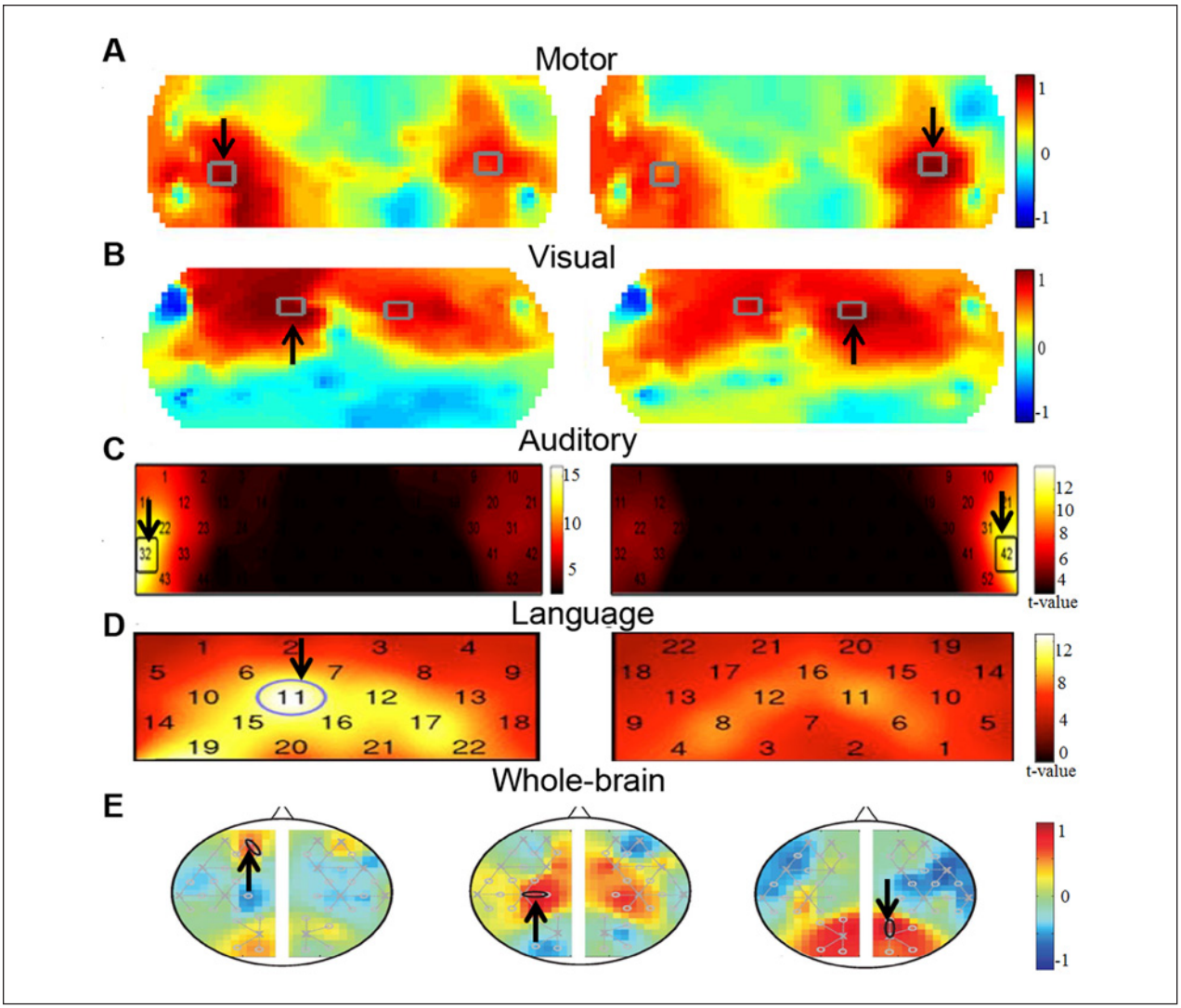

Figure 2. Seed-based correlation analysis. The resting-state functional connectivity (RSFC) map was produced separately from the (A) motor regions (White and others 2009), (B) visual regions (White and others 2009), (C) auditory regions (Lu and others 2010), (D) language systems (Y-J Zhang and others 2010), and (E) entire brain (Mesquita and others 2010). The RSFC maps in (A-C) represent the correlation calculated from left and right hemispheric seeds (black arrows), respectively. The RSFC maps in (D, E) represented the correlation from the given seeds (black arrows), respectively. Note that the numbers in (C) and (D) represent the indices of the measurement channels in the probe and the color bar represents the statistical values such as correlation coefficient or *t* values.

consistent with that determined from both a data-driven cluster analysis and a predefined template in the auditory regions. Also using the seed-correlation analysis strategy, this research group found strong functional connectivity within the bilateral language system (Y-J Zhang and others 2010), further confirming the feasibility of using R-fNIRS to detect RSFC in high-level functional brain systems. In whole-head functional network studies, the seed-correlation approach was also shown to be capable of identifying multiple functional brain networks from the whole-brain data set. The corresponding study was performed by Mesquita and others (2010), who simultaneously recorded brain signal in regions of the frontal, parietal, temporal and occipital cortices of each participant. The seed point in each functional brain system was separately localized and then used as the correlation analysis of the whole-brain data. Each identified functional system corresponded to a functional connectivity network, more often evidently for the sensorimotor and visual networks, further highlighting the feasibility of using functional connectivity and optical methods to investigate cortical interactions within the entire brain system.

Independent component analysis. Independent component analysis is a statistical approach that was designed to extract independent sources from a data set of mixed and unknown sources. ICA was originally proposed as a blind source separation method (Hyvärinen 1999) and is now increasingly used to remove noise (Kohno and others 2007; McKeown and others 2003; Srivastava and others 2005; Thomas and others 2002) and detect functional connectivity (Greicius and others 2004; Iriarte and others 2003; Kiviniemi and others 2003; Scheeringa and others 2008; van de Ven and others 2004; H. Zhang and others 2010) in fMRI/EEG/fNIRS data. H. Zhang and others (2010) recently applied the ICA algorithm to R-fNIRS to identify RSFC in the motor and visual cortices, which was previously accomplished using the seed-correlation method. Temporal ICA analysis was performed on a series of R-fNIRS data (from 21 young adults) by assuming the temporal independence of the unknown signal sources. The decomposed components of interest (i.e., the sensorimotor and visual components) were visually identified according to the spatial map of the component and the frequency power of its time course. Generally, RSFC maps showed localized and symmetrical spatial distribution in either the motor or the visual system, and the correlation maps were also established to be consistent with the spatial maps from the seed correlation approaches and with the predefined labeling map in the motor or visual areas (Fig. 3). A similar ICA analysis was conducted by White and others (2012) to identify visual RSFC in healthy newborn infants and in newborn infants with occipital strokes. In the healthy newborns, bilateral functional connectivity in the visual cortex was effectively identified using the ICA method; in contrast, abnormal unilateral connectivity patterns in visual cortex were identified in the infants with the occipital strokes. The results of these two ICA studies (White and others 2012; H. Zhang and others 2010) demonstrate the feasibility of ICA for use in R-fNIRS RSFC detection.

Whole-brain correlation analysis. Whole-brain correlation analysis represents the computation of the functional connectivity between any two measurement channel pairs in the whole brain. Using this method, Homae and others (2010) demonstrated that RSFC of human infants from several days to 6 months after birth varies dynamically along the developmental course. Zhang and others (2012) also used this method to show that the dominant frequency of RSFC within one functional system can be identified by introducing anatomical priori information about this functional system. For different brain regions of functional systems, Sasai and others (2011) found that the global properties of RSFC are also frequency dependent. To address this frequency-dependent phenomenon, they first decomposed the hemodynamic fluctuations

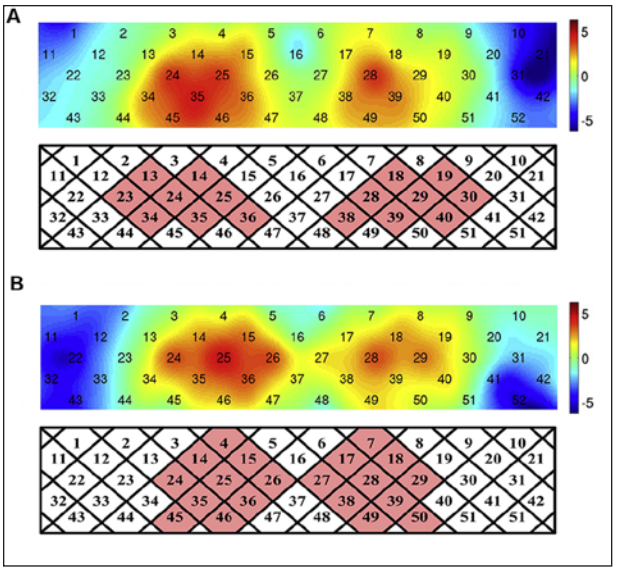

Figure 3. Independent component analysis–derived resting-state functional connectivity (RSFC) maps (H. Zhang and others 2010). The maps for (A) sensorimotor system and (B) visual system. The probe holder with same configuration was separately positioned above the sensorimotor and visual areas during data collection. The labeling map for each functional system is shown below the RSFC map, with red indicating channels above the bilateral motor or visual areas. The spatial patterns of the RSFC map show a localized and symmetrical distribution, which highly resembled the labeling map of the motor or visual system.

recorded from multiple regions of prefrontal, temporal, and occipital cortex during the resting state into various frequency bands (0.009-0.02, 0.02-0.04, 0.04-0.06, 0.06-0.08, and 0.08-0.1 Hz). Then the whole-brain RSFC between any two channels were calculated on each frequency band. Functional connections with correlation coefficients greater than 0.6 were considered to be edges. The results showed that edges between homologous cortical regions showed high correlation over a wide frequency range (0.009-0.1 Hz) (Fig. 4), which could be due to direct neuroanatomical connections between homologous regions. However, edges between the frontal and occipital regions exhibited frequency-specific functional connectivity in a narrow frequency range (0.04-0.1 Hz) (Fig. 4). This narrow frequency corresponded to the time scale of typical hemodynamic response to a single event, and the connections may thus reflect synchronization of transient neural activation among distant cortical regions.

Graph-theoretical analysis. The graph-theory approach is a straightforward and powerful tool for characterizing the topological architecture of brain networks. Using this approach, a variety of neuroimaging (e.g., fMRI and EEG/MEG) research has shown that the human

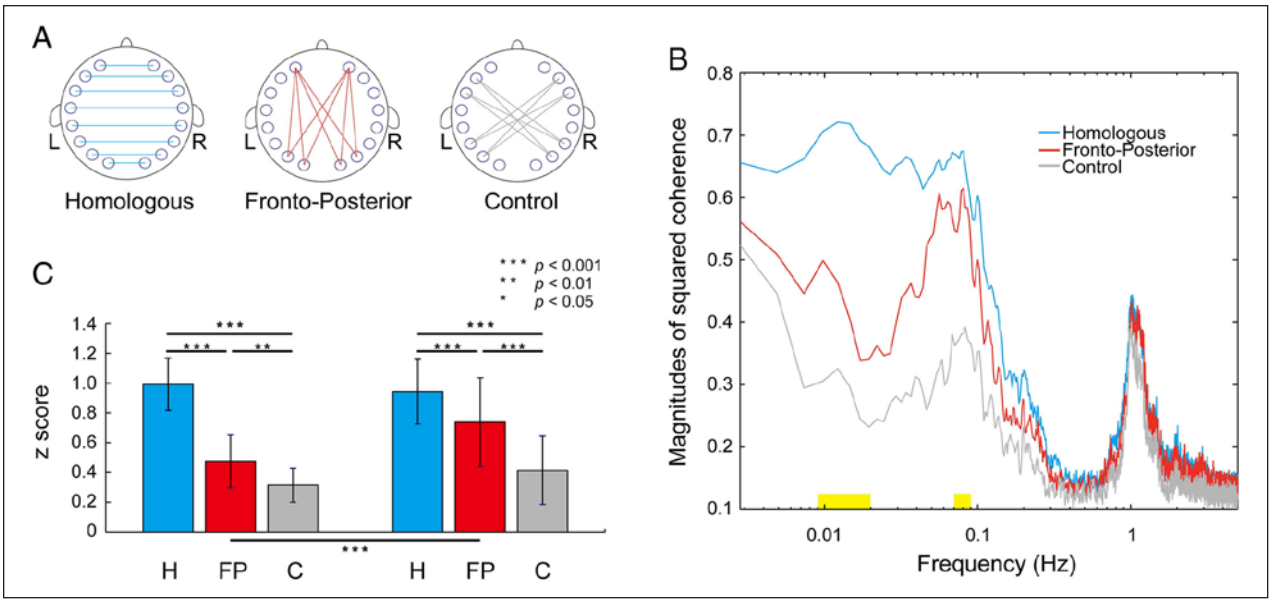

Figure 4. The averaged squared coherence for the connectivity group using whole-brain correlation analysis (Sasai and others 2011). (A) The configurations of selected connectivity groups. (B) Magnitudes of participant averaged squared coherence for each connectivity group. Yellow bars indicate the range of very low frequency (VLF) (0.009-0.02 Hz) and low frequency (LF) (0.06-0.08 Hz). (C) Statistical analysis results using a two-way analysis of variance (factor 1, connectivity groups; factor 2, frequency bands). Bars show the individual correlation data normalized to the z scores by using Fischer's z transformation. The terms "H," "FP," and "C" represent homologous, frontoposterior, and control connectivity, respectively. The error bars indicate the standard deviations. Significant differences between the connectivity groups and between the frequency bands are shown (*$P < 0.05$, **$P < 0.01$, ***$P < 0.001$, post hoc tests).

brain network is topologically organized in a non-trivial manner (e.g., with small-world architecture and modular structures) that supports efficient information processing in the brain (Bullmore and Sporns 2009; He and Evans 2010; Stam 2010; Yu and others 2011; Zalesky and others 2012). Recently, Niu and others (2012) used the graph-theoretical network analysis approach to examine the topological organization of the human whole-brain functional network constructed using R-fNIRS data. In the R-fNIRS brain network framework, the channels are considered to be vertices, and the functional connections between the channels are considered to be edges. Therefore, R-fNIRS data with N nodes formed an $N \times N$ correlation matrix, in which each value represents the functional connectivity between nodes. The functional connectivity was obtained by computing the Pearson correlation coefficients for the time series between pairs of nodes. Furthermore, the correlation matrix was thresholded into a binary graph, such that edges with absolute connectivity strengths larger than the threshold value were set to 1 and all others were set to 0. Finally, a series of graphic metrics of topological networks were applied to characterize the R-fNIRS functional brain network. Overall, the authors found that the network properties derived from the R-fNIRS data were consistent with previous findings from other imaging techniques (e.g., fMRI and EEG/MEG), exhibiting modularity, small-worldness, and the existence of highly connected network hubs (Fig. 5). The network properties were also relatively consistent between the individual networks and the population-based mean networks. This study represents the first topological investigation of whole-brain functional connectivity network using graph-theory combined with R-fNIRS. Notably, based on one single functional brain system (i.e., the motor system), Duan and others (2012) calculated two network parameters (the clustering coefficient and the characteristic path length) using graph theoretical analysis and found that these two parameter values derived from R-fNIRS data were compatible with those derived from the fMRI data. Thus, these two studies (Duan and others 2012; Niu and others 2012) demonstrated that a combination of graph-theory approaches and optical imaging techniques is feasible for the exploration of the topological organization of human brain functional networks. Notably, compared with the above-mentioned three RSFC approaches (seed-based correlation analysis, ICA, and whole-brain correlation analysis) that focus on the relationship between individual regions or separate components, the graph theory-based approach primarily focuses on revealing the topological principles governing the functional connectivity patterns within the whole-brain network.

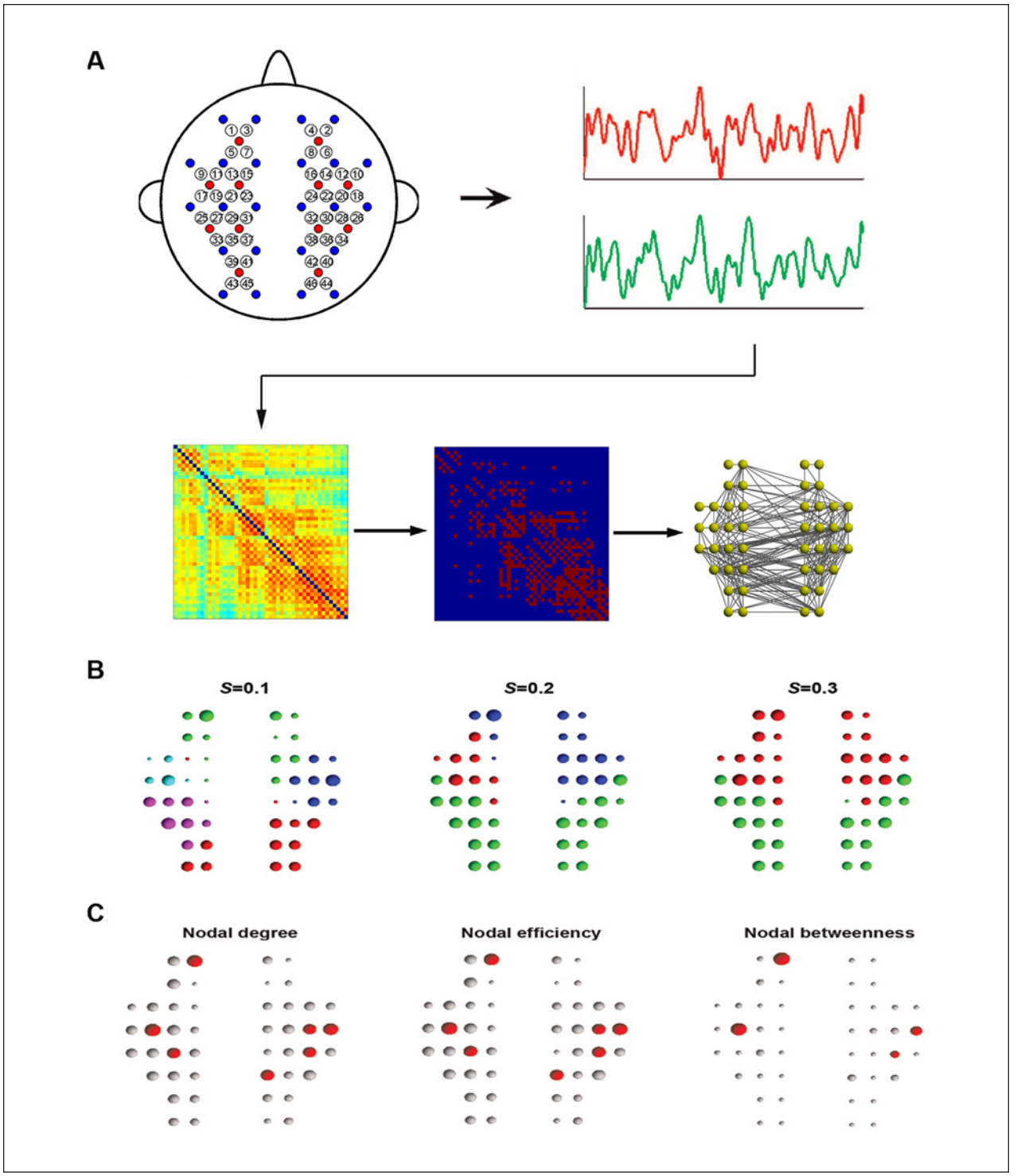

Figure 5. Graph-theoretical topological analysis (Niu and others 2012). (A) Flowchart for the construction of a functional brain network. (B) Modular architectures of functional networks at several selective sparsity thresholds (0.1, 0.2, and 0.3). Five, three, and two functional modules are separately identified in the functional brain network. The size of each node denotes its relative nodal degree value in the brain network. (C) Hubs (red) in the functional brain network. The node size indicates its relative nodal centrality normalized to the corresponding mean for all nodes in the network.

Assessment of RSFC Performance

Notably, a number of factors could influence the detection performance of an R-fNIRS brain network, such as variations in the fNIRS instruments and measurement environment (Leff and others 2011), in the probe placement across participants and scanning sessions (Hoshi 2007), and in the participants' mental states during scanning (Shehzad and others 2009). Consequently, reliability, reproducibility, and validity, which are important for fNIRS-based RSFC studies in basic and clinical neuroscience, have been examined in several recent R-fNIRS studies.

Reliability assessment. Test–retest is a general measure to examine reliability in neuroimaging studies. Usually, the test–retest involves the scanning of the data several times (e.g., twice) at different times and then researchers can compute the statistical similarity of the results with an intraclass correlation coefficient (*ICC*) (Shrout and Fleiss 1979). Using the test–retest reliability-assessment strategy, Zhang and others (2011) separately examined the reliability level of RSFC maps derived from seed-correlation and ICA-derived approaches. The scanning interval for two R-fNIRS recording sessions is one week. The reliability results of the RSFC analysis using these two different approaches consistently demonstrated that fNIRS-based RSFC is reliable, independent of the individual and group levels determined by spatial map and functionally connected clusters. Recently, Niu and others (2013) used R-fNIRS and a graph-theoretical approach to systematically address test–retest reliability of human brain functional networks, including RSFCs, global network metrics and regional nodal centrality metrics. Eighteen subjects participated in two R-fNIRS scan sessions held ~20 minutes apart. Functional brain networks were constructed for each subject by computing temporal correlations on three types of hemoglobin concentration information (HbO, HbR, and HbT), followed by a graph-theoretical analysis. An *ICC* was further applied to quantify the test–retest reliability of each network metric. They observed that a large proportion of RSFCs (~90%) exhibited good reliability ($0.6 < ICC < 0.74$). For global and nodal measures, reliability was generally threshold sensitive and varied between both network metrics and hemoglobin concentration signals. Specifically, the majority of global metrics exhibited fair to excellent reliability, with notably higher *ICC* values for the clustering coefficient (HbO, 0.76; HbR, 0.78; HbT, 0.53) and global efficiency (HbO, 0.76; HbR, 0.70; HbT, 0.78). Similarly, both nodal degree and efficiency measures also showed fair to excellent reliability across nodes (degree, 0.52-0.84; efficiency, 0.50-0.84); reliability was concordant across HbO, HbR and HbT and was significantly higher than that of nodal betweenness (0.28-0.68). Together, these results suggest that many graphic metrics derived from R-fNIRS are test–retest reliable and can be used for brain network research.

Reproducibility assessment. Niu and others (2011) demonstrated the reproducibility of RSFC maps between systems by repeating similar experiments using different instruments (DYNOT and CW5). The experimental protocol used in this study was the same as that used in the study by Lu and others (2010), so these results provided a direct RSFC comparison between different research groups. A similar analysis strategy (seed-based correlation) to that used in Lu and others' study was adopted to identify the RSFC in the motor regions of each dataset. For each data set, the bilateral motor regions showed the strongest functional connectivity, and the spatial connectivity maps also showed similar patterns of spatial distribution between the two imaging systems and between the research groups. Taken together, this evidence suggests that fNIRS-based RSFC detection is reproducible in other imaging systems and research groups, allowing fNIRS researchers to confidently use different fNIRS instruments for RSFC detection in the future. Moreover, Niu and others (2012) also investigated the reproducibility of the graphic topological properties of the R-fNIRS brain network using a splitting-half analysis across participants and over time. Specifically, they divided all participants into two nonoverlapping subgroups and also further divided the entire dataset into two equal parts to examine the reproducibility of the network metrics both across subjects and over time. For each subgroup and each sub–data set, the authors constructed an adjacent matrix, with which they analyzed and compared the topological properties of the constructed functional brain networks. The compared results showed high consistency and good similarity between network properties of each data set, indicating that the fNIRS-based, graph theory–derived topological properties of human brain networks are stable and highly reproducible across subjects and over time.

Validity assessment. Given that fMRI is generally considered an important reference technique for in vivo imaging of human brain activity, one way of demonstrating the validity of fNIRS-based RSFC detection is to compare fNIRS and fMRI results using either simultaneous or nonsimultaneous data collection. For example, White and others (2009) conducted nonsimultaneous data acquisition of fNIRS and fMRI signals on one subject and found that the spatial RSFC maps between these two modalities were quantitatively similar in both the motor and the visual brain regions. Furthermore, based on the simultaneous acquisition signals from the fNIRS in bilateral motor regions and the fMRI in the whole brain, Duan and

others (2012) found that fNIRS and fMRI produce comparable RSFC patterns, demonstrating the validity of R-fNIRS RSFC detection in local brain regions. Moreover, in the whole-brain range, Sasai and others (2012) found that using fNIRS signal as a seed point to correlate the whole-brain blood oxygen level–dependent (BOLD) signal can accurately identify three known resting-state networks (the dorsal attention, the frontoparietal control, and the default mode networks). These networks were shown to be comparable to the resting-state networks that use the BOLD signal as a seed point to correlate with the whole-brain BOLD signal, thus confirming the validity of RSFC detection for use in the whole-brain range. Although different spatial correspondence strategies and imaging areas were used in the studies from Duan and others (2012) and Sasai and others (2012), their fNIRS and fMRI results showed quantitative and comparable consistencies that demonstrated the validity of fNIRS-based RSFC detection.

Application of RSFC

In the fMRI field, RSFC has been demonstrated to be a potential biomarker for the assessment of brain states in healthy and diseased populations (Bassett and others 2009; van den Heuvel and Hulshoff Pol 2010; Xia and He 2011). In the fNIRS community, such a RSFC approach has also been used to characterize brain connectivity changes with development (Homae and others 2010) and disease (White and others 2012). For example, based on whole-brain data acquisition from a group of 52 healthy infants between several days and 6 months of age, Homae and others (2010) found that the cortical network organization showed regional dependency and dynamic changes during development (Fig. 6). Specifically, the temporal, parietal, and occipital cortical regions showed an increased connectivity pattern, whereas the frontal regions showed a remarkable decrease in connectivity. This finding reflects the strengthening and pruning of connections between corresponding cortical regions during the development of the infant brain. In addition, the number of frontoposterior long-connectivity interactions decreased from the neonatal period to the age of 3 months and increased from the age of 3 months to the age of 6 months. This "U-shaped" pattern observed over the first 6 months may demonstrate a reorganization of the connectivity between the frontal and posterior regions during development (Fig. 6). This literature is the first R-fNIRS study to explore developmental changes in the functional connectivity of early infants. Moreover, White and others (2012) also showed that functional connectivity can be acquired at the bedside in the nursery and in neonatal intensive care units using optical methods (Fig. 7). In particular, the authors found that the functional connectivity within the visual network in an infant with unilateral occipital stroke was unilateral and nonsymmetrical, according to both the seed-correlation method and the ICA approach. This is remarkably different from the functional connectivity pattern of healthy infants, in which the spatial patterns of connectivity that map to the occipital brain regions display a strong, bilaterally symmetrical connectivity. This study represents the first optical resting-state network in disordered infants, demonstrating the promise of fNIRS-based RSFC for use in a clinical setting.

Future Perspectives

In this review, we summarized the recent advances made in RSFC study of spontaneous brain activity in the R-fNIRS field. These distinct RSFC analysis methodologies (e.g., the seed-based correlation analysis, ICA, whole-brain correlation analysis and graph-theoretical topological analysis) have all been successfully applied to R-fNIRS data and have achieved many significant results. These findings provide crucial evidence to demonstrate the feasibility and validity of the fNIRS technique for the study of resting-state brain networks. More important, these findings have increased our understanding of the intrinsic human brain connectivity networks, as derived from R-fNIRS. However, studies on the fNIRS-based human brain functional networks are still in their early stages, and many challenging issues in this new research field need to be addressed through future work.

First, although functional connectivity can be characterized by different methods, such as seed-based correlation and ICA-derived analysis, it is not known which method can best describe the intrinsic functional connectivity of the brain. Moreover, with the application of graph theoretical approaches for R-fNIRS, it remains to be determined if the definition of network nodes and edges used in fMRI are also suitable for use in R-fNIRS. In addition, although a number of different strategies for analyzing fNIRS data have been proposed, no unified standard has emerged for the analysis of R-fNIRS data, which may produce biased results and conclusions. For example, in terms of the robust hemoglobin concentration used to characterize functional connectivity during the resting state, several research groups have identified nonconforming patterns (Duan and others 2012; Homae and others 2010; Lu and others 2010; Mesquita and others 2010; Niu and others 2011; White and others 2009; H. Zhang and others 2010). There also exist competitive disputes concerning the major components of low-frequency R-fNIRS signals. For example, Tong and Frederick (2010) found that the low-frequency components of the R-fNIRS signals were affected by fluctuations in blood flow and hemoglobin oxygenation at a

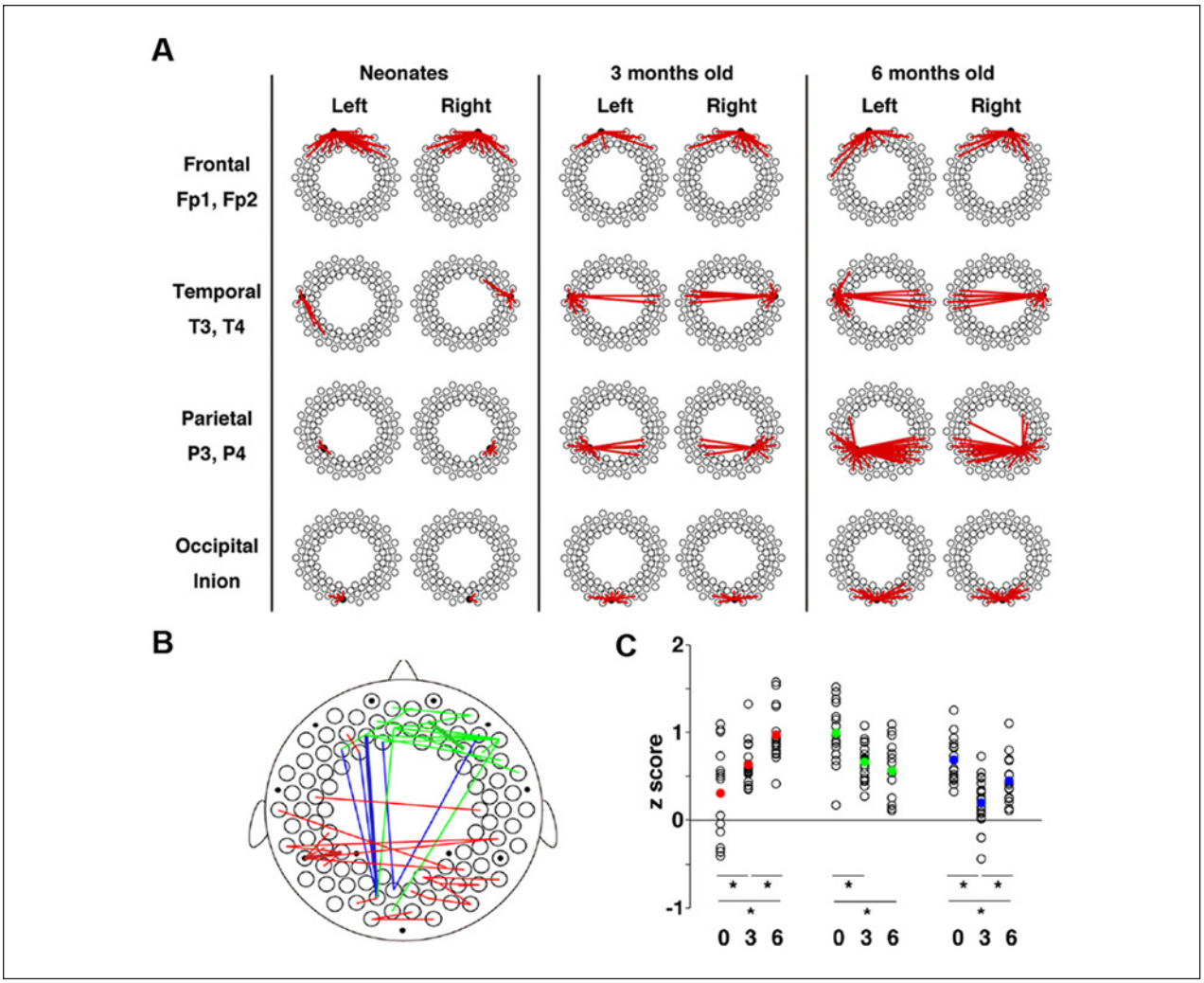

Figure 6. Developmental changes of resting-state functional connectivity (RSFC) in early infancy (Homae and others 2010). (A) Representative distribution of correlation coefficients. The red lines show correlations greater than 0.5. (B, C) Increases, decreases, and U-shaped changes in connectivity during the course of development. The red, green, and blue lines in (B) connect channels that showed significant changes in temporal correlations. (C) Individual correlation data normalized to the *z* scores by using Fischer's *z* transformation. The data for connections shown by the bold lines in (B) are presented here. The differences between the infant groups are shown (*$P < 0.05$, post hoc tests, Tukey's honestly significant difference).

global circulatory system level. Conversely, Sasai and others (2012) noted that the low-frequency R-fNIRS signals mainly contained information representing spontaneous cortical activity, although some physiological noise from non-brain tissues was aliased to the signal. These differences primarily originate from the distinct processing methods and analysis strategies that were applied in these studies. Therefore, it is critical to develop a set of standard resting-state data analysis methods to facilitate the use of fNIRS in future brain functional network studies.

Second, although graph theoretical brain network analysis has attracted a great deal of attention and has proven feasible for R-fNIRS study, the reliability and reproducibility of the graph metrics of functional human brain networks derived from this technique remain to be elucidated. Some experimental factors could affect the reliability of graphic metrics of the R-fNIRS brain network, including the fNIRS instruments and measurement environment (Leff and others 2011), the probe placement across participants and scanning sessions (Hoshi 2007), and the participants' mental states (Shehzad and others 2009). Given these concerns, it is important and necessary to systematically study the test–retest reliability of graphic properties of R-fNIRS brain networks. If these metrics are test–retest reliable, they have the potential to be adopted for use as biomarkers in future cognitive neuroscience and clinical research, especially in longitudinal

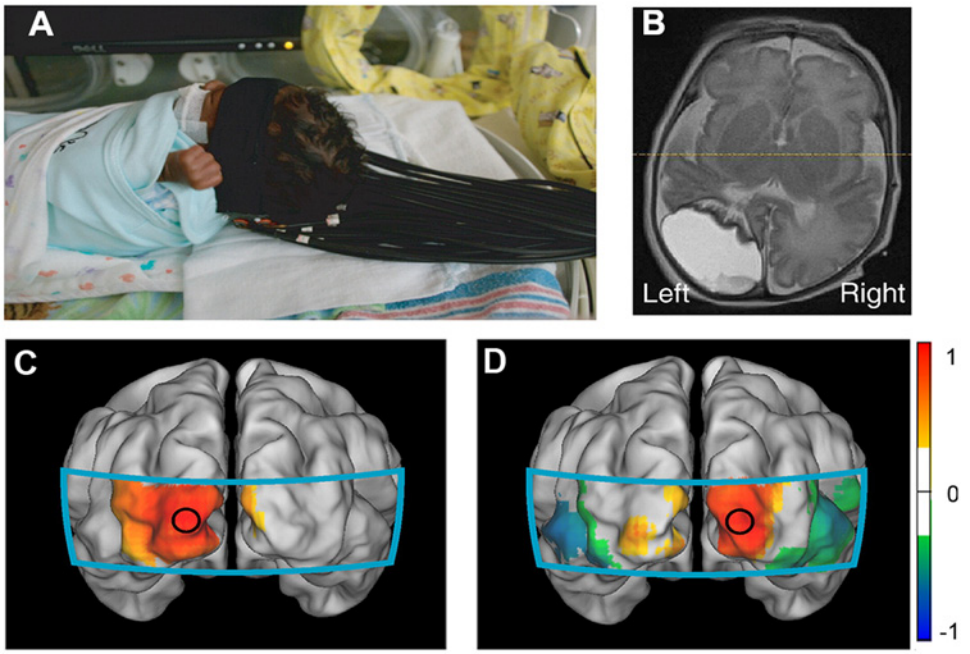

Figure 7. Bedside resting-state functional connectivity (RSFC) detection in infants (White and others 2012). (A) Photograph of the optical probe on a premature infant. (B) An axial slice (neurological orientation) of a T2-weighted MRI in a preterm infant with an occipital stroke. (C, D) RSFC maps using seeds placed where the left and right visual cortices are expected to be. In both cases, only unilateral correlations were found.

studies of brain changes and in research using repeated measurements in the context of normal development or pharmacological treatments.

Third, what are the origins of detected brain functions or, more generally, how to quantify the separate contributions of the neural and nonneural activities? Theoretically, one could raise the importance of multimodal imaging to unravel the origins of detected brain fluctuations. New developments like magnetic resonance encephalography (Hennig 2012; Zahneisen and others 2012) and other inverse imaging techniques (Boyacioğlu and Barth 2012; Lin and others 2012) make the detection and sampling of brain activity fluctuations more precise but also more noisy. In contrast to those imaging techniques, fNIRS exhibited its particular advantages of low instrumental noise, clear physiological significance of the measured hemoglobin signals and free of electromagnetic interference as well as the merits of low physical burden for subjects, good portability, and relatively high temporal sampling rate. Therefore, fNIRS is considered to be a potential neuroimaging technique to unravel the origins of detected brain fluctuations with the combination of other imaging modalities. Specifically, recent studies have shown that the utility of fNIRS signal simultaneously measured with other neuroimaging technique (e.g., fMRI) is useful for partitioning the contributing factors of the low-frequency physiological noises (Tong and others 2011) as well as regressing out these noise components with fNIRS (Cooper and others 2012; Frederick and others 2012).

Fourth, constructing dynamic human brain networks and understanding potential time-varying network behaviors is a significant goal for future R-fNIRS studies. The human brain is a complex and dynamic system, and its dynamic nature may be even more prominent in a resting state with unconstrained mental activity. Recent resting-state studies using fMRI and EEG/MEG have consistently demonstrated that the spontaneous functional connectivity network exhibits dynamic changes within time scales of seconds to minutes (Allen and others 2012; Chang and Glover 2010; Kang and others 2011). Additionally, several task- or stimuli–response–based studies have demonstrated that functional brain networks exhibit task-induced changes in the topology features of the functional networks. For instance, Kitzbichler and others (2011) found that human brain functional systems can immediately reconfigure the efficiency of brain networks according to the load of cognitive engagement. Therefore, exploring the dynamics of functional brain connectivity networks may reveal

intrinsic information about the processing mechanisms of the human brain and capture variability that could provide novel insights into functional connectivity differences found in various neuropsychiatric diseases (Xia and He 2011). Given that fNIRS can also provide the measures of brain metabolism in addition to hemoglobin-based information (Heekeren and others 1999; Jobsis 1977; Obrig 2013), it will also be significant and promising to investigate the dynamic brain mechanism with fNIRS. For example, by recording data from several wavelengths simultaneously, one can measure different tissue chromophores such as cytochrome *c* and cytochrome oxidase (i.e., cytochrome *aa3*) (Strangman and others 2002; Yin and others 2013). As a marker of metabolic demands, cytochrome *aa3* measurements can provide more direct information about neuronal activity than hemoglobin changes (Heekeren and others 1999; Jobsis 1977). There is also evidence to show that fNIRS can detect fast signal occurring in the 50 to 200 ms following neuronal firing (Gratton and Fabiani 2001; Steinbrink and others 2000; Stepnoski and others 1991). However, in the application to human brain function studies, two notable challenges exist for the cytochrome *aa3*, primarily involving the technical complexities associated with this measurement in the human brain and the insufficient chromophore separation algorithm (Cooper and others 1999; Cooper and Springett 1997). Notably, a hybrid optical spectrometer and accompanying algorithm designed to address the above issues has recently been developed by Clare E. Elwell's group. (Kolyva and others 2012; Tachtsidis and others 2010). Based on the instrument and theory, they found that the change of cytochrome *aa3* was a better brain-specific signal of cerebral metabolism compared to hemoglobin information (Kolyva and others 2013), which therefore fortifies its clinical appeal as a noninvasive marker of regional cerebral metabolic status in future.

Fifth, we still know very little about how resting-state functional brain networks relate to individual traits. The answer to this question may provide new insights into understanding the differences and relationships between the brain functional networks of different individuals. Using fMRI, van den Heuvel and others (2009) found that the overall organization of spontaneous functional brain networks had a strong negative correlation between the normalized characteristic path length and the intelligence quotient. Additionally, Smit and others (2008) demonstrated that individual differences in the topological properties of resting-state functional brain networks are heritable. It will therefore be of significant interest to investigate the relationship between network organization and individual characteristics (e.g., intelligence quotient and memory or attention abilities) in the context of R-fNIRS on persons such as young children and patients with severe movement disorders.

Finally, there are currently only a few studies focusing on functional connectivity attributes during the performance of tasks. For example, Najafizadeh and others (as cited in Fan and others 2013) conducted a preliminary fNIRS study and found that the prefrontal cortex RSFC differed before and after executing a working memory task. Eguíluz and others (2005) reported that scale-free small-world topology in human brain networks remained constant between different task conditions. Bassett and others (2006) also found that the behavioral state during task performance did not strongly influence the global topology of the human brain network at rest, but that was instead associated with the emergence of some long-range connections. This group (Bassett and others 2009) further confirmed that good working memory task performance was positively correlated with the cost-efficiency of the beta-band brain networks. Collectively, these investigations suggest that studying brain networks under both resting and task conditions and during the transition between these states may offer new insights into the rapid adaptive reconfiguration of neuronal assemblies that underlie the changes between cognitive states.

Conclusions

This review demonstrates the current advances on the fNIRS-based RSFC literature by highlighting the progression from RSFC detection methodologies (e.g., seed-based correlation analysis, ICA, whole-brain correlation analysis and graph-theoretical topological analysis), RSFC performance assessment (e.g., its reliability, reproducibility, and validity) to recent RSFC applications. An accumulating body of evidence suggests that R-fNIRS is a valid tool for the exploration of RSFC in normal and diseased conditions. It is certain that more research will be needed before R-fNIRS can be used in comprehensive and reliable investigations of functional brain connectivity patterns. These efforts are introducing new avenues of research on the organizational mechanisms of the brain that will be of interest to all basic scientists and clinical researchers.

Acknowledgments

We would like to thank Zhen Li and Jingping Xu for the figure preparation, and American Journal Experts (http://www.journalexperts.com/) for their English editing and proofreading.

Declaration of Conflicting Interests

The author(s) declared no potential conflicts of interest with respect to the research, authorship, and/or publication of this article.

Funding

The author(s) disclosed receipt of the following financial support for the research, authorship, and/or publication of this article: This work was supported by the Natural Science Foundation of China (Grant Nos. 81201122, 81030028 and 31221003), the National Science Fund for Distinguished Young Scholars (Grant No. 81225012), the Fundamental Research Funds for the Central Universities (Grant No. 2012LYB06), the Specialized Research Fund for the Doctoral Program of Higher Education, Beijing Natural Science Foundation (Grant No. Z111107067311036), the Beijing Funding for Training Talents (YH) and Major Project of National Social Science Foundation (Grant No. 11&ZD186).

References

Allen EA, Damaraju E, Plis SM, Erhardt EB, Eichele T, Calhoun VD. 2012. Tracking whole-brain connectivity dynamics in the resting state. Cereb Cortex. Nov 11 [Epub ahead of print]

Arridge SR, Cope M, Delpy D. 1992. The theoretical basis for the determination of optical pathlengths in tissue: temporal and frequency analysis. Phys Med Biol 37(7):1531–60.

Bassett DS, Bullmore ET. 2009. Human brain networks in health and disease. Curr Opin Neurol 22(4):340–7.

Bassett DS, Bullmore ET, Meyer-Lindenberg A, Apud JA, Weinberger DR, Coppola R. 2009. Cognitive fitness of cost-efficient brain functional networks. Proc Natl Acad Sci U S A 106(28):11747–52.

Bassett DS, Gazzaniga MS. 2011. Understanding complexity in the human brain. Trends Cogn Sci 15(5):200–9.

Bassett DS, Meyer-Lindenberg A, Achard S, Duke T, Bullmore E. 2006. Adaptive reconfiguration of fractal small-world human brain functional networks. Proc Natl Acad Sci U S A 103(51):19518–23.

Boas DA, Dale AM, Franceschini MA. 2004. Diffuse optical imaging of brain activation: approaches to optimizing image sensitivity, resolution, and accuracy. Neuroimage 23(Suppl 1):S275–88.

Boyacioğlu R, Barth M. 2012. Generalized iNverse imaging (GIN): ultrafast fMRI with physiological noise correction. Magn Reson Med. Oct 24 [Epub ahead of print]

Bullmore E, Sporns O. 2009. Complex brain networks: graph theoretical analysis of structural and functional systems. Nat Rev Neurosci 10(3):186–98.

Chang C, Glover G. 2010. Time–frequency dynamics of resting-state brain connectivity measured with fMRI. Neuroimage 50(1):81–98.

Cooper CE, Cope M, Springett R, Amess PN, Penrice J, Tyszczuk L, and others. 1999. Use of mitochondrial inhibitors to demonstrate that cytochrome oxidase near-infrared spectroscopy can measure mitochondrial dysfunction noninvasively in the brain. J Cereb Blood Flow Metab 19(1):27–38.

Cooper CE, Springett R. 1997. Measurement of cytochrome oxidase and mitochondrial energetics by near–infrared spectroscopy. Philos Trans R Soc Lond B Biol Sci 352(1354):669–76.

Cooper RJ, Gagnon L, Goldenholz DM, Boas DA, Greve DN. 2012. The utility of near-infrared spectroscopy in the regression of low-frequency physiological noise from functional magnetic resonance imaging data. Neuroimage 59(4):3128–38.

Cope M, Delpy D. 1988. System for long-term measurement of cerebral blood and tissue oxygenation on newborn infants by near infra-red transillumination. Med Biol Eng Comput 26(3):289–94.

Delpy DT, Cope M, Van der Zee P, Arridge S, Wray S, Wyatt J. 1988. Estimation of optical pathlength through tissue from direct time of flight measurement. Phys Med Biol 33(12):1433–42.

Duan L, Zhang Y-J, Zhu C-Z. 2012. Quantitative comparison of resting-state functional connectivity derived from fNIRS and fMRI: a simultaneous recording study. Neuroimage 60(4):2008–18.

Eguíluz VM, Chialvo DR, Cecchi GA, Baliki M, Apkarian AV. 2005. Scale-free brain functional networks. Phys Rev Lett 94(1):018102.

Fan F, Zhu C, Chen H, Qin W, Ji X, Wang L, and others. 2013. Dynamic brain structural changes after left hemisphere subcortical stroke. Hum Brain Mapp 34(8):1872–81.

Ferrari M, Quaresima V. 2012. A brief review on the history of human functional near-infrared spectroscopy (fNIRS) development and fields of application. Neuroimage 63(2):921–35.

Fox MD, Raichle ME. 2007. Spontaneous fluctuations in brain activity observed with functional magnetic resonance imaging. Nat Rev Neurosci 8(9):700–11.

Frederick BD, Nickerson LD, Tong Y. 2012. Physiological denoising of BOLD fMRI data using regressor interpolation at progressive time delays (RIPTiDe) processing of concurrent fMRI and near-infrared spectroscopy (NIRS). Neuroimage 60(3):1913–23.

Gervain J, Macagno F, Cogoi S, Peña M, Mehler J. 2008. The neonate brain detects speech structure. Proc Natl Acad Sci U S A 105(37):14222–7.

Gratton G, Fabiani M. 2001. Shedding light on brain function: the event-related optical signal. Trends Cogn Sci 5(8):357–63.

Greicius MD, Srivastava G, Reiss AL, Menon V. 2004. Default-mode network activity distinguishes Alzheimer's disease from healthy aging: evidence from functional MRI. Proc Natl Acad Sci U S A 101(13):4637–42.

He Y, Evans A. 2010. Graph theoretical modeling of brain connectivity. Curr Opin Neurol 23(4):341–50.

Heekeren HR, Kohl M, Obrig H, Wenzel R, von Pannwitz W, Matcher SJ, and others. 1999. Noninvasive assessment of changes in cytochrome-c oxidase oxidation in human subjects during visual stimulation. J Cereb Blood Flow Metab 19(6):592–603.

Hennig J. 2012. Functional spectroscopy to no-gradient fMRI. Neuroimage 62(2):693–8.

Homae F, Watanabe H, Otobe T, Nakano T, Go T, Konishi Y, and others. 2010. Development of global cortical networks in early infancy. J Neurosci 30(14):4877–82.

Hoshi Y. 2007. Functional near-infrared spectroscopy: current status and future prospects. J Biomed Opt 12(6):062106.

Hyvärinen A. 1999. Fast and robust fixed-point algorithms for independent component analysis. IEEE Trans Neural Netw 10(3):626–34.

Iriarte J, Urrestarazu E, Valencia M, Alegre M, Malanda A, Viteri C, and others. 2003. Independent component analysis as a tool to eliminate artifacts in EEG: a quantitative study. J Clin Neurophysiol 20(4):249–57.

Jobsis F. 1977. Noninvasive, infrared monitoring of cerebral and myocardial oxygen sufficiency and circulatory parameters. Science 198(4323):1264–7.

Kang J, Wang L, Yan C, Wang J, Liang X, He Y. 2011. Characterizing dynamic functional connectivity in the resting brain using variable parameter regression and Kalman filtering approaches. Neuroimage 56(3):1222–34.

Kitzbichler MG, Henson RN, Smith ML, Nathan PJ, Bullmore ET. 2011. Cognitive effort drives workspace configuration of human brain functional networks. J Neurosci 31(22):8259–70.

Kiviniemi V, Kantola J-H, Jauhiainen J, Hyvärinen A, Tervonen O. 2003. Independent component analysis of nondeterministic fMRI signal sources. Neuroimage 19(2):253–60.

Kohno S, Miyai I, Seiyama A, Oda I, Ishikawa A, Tsuneishi S, and others. 2007. Removal of the skin blood flow artifact in functional near-infrared spectroscopic imaging data through independent component analysis. J Biomed Opt 12(6):062111.

Kolyva C, Ghosh A, Tachtsidis I, Highton D, Cooper CE, Smith M, and others. 2013. Cytochrome *c* oxidase response to changes in cerebral oxygen delivery in the adult brain shows higher brain-specificity than haemoglobin. Neuroimage. May 23 [Epub ahead of print]

Kolyva C, Tachtsidis I, Ghosh A, Moroz T, Cooper CE, Smith M, and others. 2012. Systematic investigation of changes in oxidized cerebral cytochrome c oxidase concentration during frontal lobe activation in healthy adults. Biomed Opt Express 3(10):2550–6.

Leff DR, Orihuela-Espina F, Elwell CE, Athanasiou T, Delpy DT, Darzi AW, and others. 2011. Assessment of the cerebral cortex during motor task behaviours in adults: a systematic review of functional near infrared spectroscopy (fNIRS) studies. Neuroimage 54(4):2922–36.

Lin F-H, Tsai KW, Chu Y-H, Witzel T, Nummenmaa A, Raij T, and others. 2012. Ultrafast inverse imaging techniques for fMRI. Neuroimage 62(2):699–705.

Lu C-M, Zhang Y-J, Biswal BB, Zang Y-F, Peng D-L, Zhu C-Z. 2010. Use of fNIRS to assess resting state functional connectivity. J Neurosci Methods 186(2):242–9.

McKeown MJ, Hansen LK, Sejnowsk TJ. 2003. Independent component analysis of functional MRI: what is signal and what is noise? Curr Opin Neurobiol 13(5):620–9.

Mesquita RC, Franceschini MA, Boas DA. 2010. Resting state functional connectivity of the whole head with near-infrared spectroscopy. Biomed Opt Express 1(1):324–36.

Nakano T, Watanabe H, Homae F, Taga G. 2009. Prefrontal cortical involvement in young infants' analysis of novelty. Cereb Cortex 19(2):455–63.

Niu H, Khadka S, Tian F, Lin Z-J, Lu C, Zhu C, and others. 2011. Resting-state functional connectivity assessed with two diffuse optical tomographic systems. J Biomed Opt 16(4): 046006-5.

Niu H, Li Z, Liao X, Wang J, Zhao T, Shu N, and others. 2013. Test-retest reliability of graph metrics in functional brain networks: a resting-state fNIRS study. PLoS ONE 8(8): e72425.

Niu H, Lin Z-J, Tian F, Dhamne S, Liu H. 2010. Comprehensive investigation of three-dimensional diffuse optical tomography with depth compensation algorithm. J Biomed Opt 15(4):046005-9.

Niu H, Wang J, Zhao T, Shu N, He Y. 2012. Revealing topological organization of human brain functional networks with resting-state functional near infrared spectroscopy. PLoS One 7(9):e45771.

Obrig H. 2013. NIRS in clinical neurology—a 'promising' tool? Neuroimage. Apr 2 [Epub ahead of print]

Sasai S, Homae F, Watanabe H, Sasaki AT, Tanabe HC, Sadato N, and others. 2012. A NIRS–fMRI study of resting state network. Neuroimage 63(1):179–93.

Sasai S, Homae F, Watanabe H, Taga G. 2011. Frequency-specific functional connectivity in the brain during resting state revealed by NIRS. Neuroimage 56(1):252–7.

Scheeringa R, Bastiaansen MC, Petersson KM, Oostenveld R, Norris DG, Hagoort P. 2008. Frontal theta EEG activity correlates negatively with the default mode network in resting state. Int J Psychophysiol 67(3):242–51.

Shehzad Z, Kelly AMC, Reiss PT, Gee DG, Gotimer K, Uddin LQ, and others. 2009. The resting brain: unconstrained yet reliable. Cereb Cortex 19(10):2209–29.

Shrout PE, Fleiss JL. 1979. Intraclass correlations: uses in assessing rater reliability. Psychol Bull 86(2):420–8.

Smit DJ, Stam CJ, Posthuma D, Boomsma DI, de Geus EJ. 2008. Heritability of "small-world" networks in the brain: a graph theoretical analysis of resting-state EEG functional connectivity. Hum Brain Mapp 29(12):1368–78.

Sporns O. 2013. Network attributes for segregation and integration in the human brain. Curr Opin Neurobiol. 23(2): 162–71.

Srivastava G, Crottaz-Herbette S, Lau KM, Glover GH, Menon V. 2005. ICA-based procedures for removing ballistocardiogram artifacts from EEG data acquired in the MRI scanner. Neuroimage 24(1):50–60.

Stam CJ. 2010. Use of magnetoencephalography (MEG) to study functional brain networks in neurodegenerative disorders. J Neurol Sci 289(1-2):128–34.

Steinbrink K, Paragnik L, Jonuleit H, Tüting T, Knop J, Enk AH. 2000. Induction of dendritic cell maturation and modulation of dendritic cell-induced immune responses by prostaglandins. Arch Dermatol Res 292(9):437–45.

Stepnoski R, LaPorta A, Raccuia-Behling F, Blonder G, Slusher R, Kleinfeld D. 1991. Noninvasive detection of changes in membrane potential in cultured neurons by light scattering. Proc Natl Acad Sci U S A 88(21):9382–6.

Strangman G, Boas DA, Sutton JP. 2002. Non-invasive neuroimaging using near-infrared light. Biol Psychiatry 52(7):679–93.

Strangman G, Franceschini MA, Boas DA. 2003. Factors affecting the accuracy of near-infrared spectroscopy concentration calculations for focal changes in oxygenation parameters. Neuroimage 18(4):865–79.

Sugiura L, Ojima S, Matsuba-Kurita H, Dan I, Tsuzuki D, Katura T, and others. 2011. Sound to language: different cortical processing for first and second languages in elementary school children as revealed by a large-scale study using fNIRS. Cereb Cortex 21(10):2374–93.

Tachtsidis I, Gao L, Leung TS, Kohl-Bareis M, Cooper CE, Elwell CE. 2010. A hybrid multi-distance phase and broadband spatially resolved spectrometer and algorithm for resolving absolute concentrations of chromophores in the near-infrared light spectrum. Adv Exp Med Biol 662:169–75.

Taga G, Asakawa K, Maki A, Konishi Y, Koizumi H. 2003. Brain imaging in awake infants by near-infrared optical topography. Proc Natl Acad Sci U S A 100(19):10722–7.

Thomas CG, Harshman RA, Menon RS. 2002. Noise reduction in BOLD-based fMRI using component analysis. Neuroimage 17(3):1521–37.

Tian F, Niu H, Khan B, Alexandrakis G, Behbehani K, Liu H. 2011. Enhanced functional brain imaging by using adaptive filtering and a depth compensation algorithm in diffuse optical tomography. IEEE Trans Med Imaging 30(6):1239–51.

Tong Y, Frederick BD. 2010. Time lag dependent multimodal processing of concurrent fMRI and near-infrared spectroscopy (NIRS) data suggests a global circulatory origin for low-frequency oscillation signals in human brain. Neuroimage 53(2):553–64.

Tong Y, Lindsey KP, deB Frederick B. 2011. Partitioning of physiological noise signals in the brain with concurrent near-infrared spectroscopy and fMRI. J Cereb Blood Flow Metab 31(12):2352–62.

van de Ven VG, Formisano E, Prvulovic D, Roeder CH, Linden DEJ. 2004. Functional connectivity as revealed by spatial independent component analysis of fMRI measurements during rest. Hum Brain Mapp 22(3):165–78.

van den Heuvel MP, Hulshoff Pol HE. 2010. Exploring the brain network: a review on resting-state fMRI functional connectivity. Eur Neuropsychopharmacol 20(8):519–34.

van den Heuvel MP, Stam CJ, Kahn RS, Hulshoff Pol HE. 2009. Efficiency of functional brain networks and intellectual performance. J Neurosci 29(23):7619–24.

White BR, Liao SM, Ferradal SL, Inder TE, Culver JP. 2012. Bedside optical imaging of occipital resting-state functional connectivity in neonates. Neuroimage. 59(3):2529–38.

White BR, Snyder AZ, Cohen AL, Petersen SE, Raichle ME, Schlaggar BL, and others. 2009. Resting-state functional connectivity in the human brain revealed with diffuse optical tomography. Neuroimage 47(1):148–56.

Wray S, Cope M, Delpy DT, Wyatt JS, Reynolds EO. 1988. Characterization of the near infrared absorption spectra of cytochrome *aa3* and haemoglobin for the non-invasive monitoring of cerebral oxygenation. Biochim Biophys Acta 933(1):184–92.

Xia M, He Y. 2011. Magnetic resonance imaging and graph theoretical analysis of complex brain networks in neuropsychiatric disorders. Brain Connect 1(5):349–65.

Yin C, Zhou F, Wang Y, Luo W, Luo Q, Li P. 2013. Simultaneous detection of hemodynamics, mitochondrial metabolism and light scattering changes during cortical spreading depression in rats based on multi-spectral optical imaging. Neuroimage 76:70–80.

Yu Q, Allen EA, Sui J, Arbabshirani MR, Pearlson G, Calhoun VD. 2012. Brain connectivity networks in schizophrenia underlying resting state functional magnetic resonance imaging. Curr Top Med Chem 12(21):2415–25.

Yu Q, Plis SM, Erhardt EB, Allen EA, Sui J, Kiehl KA, and others. 2011. Modular organization of functional network connectivity in healthy controls and patients with schizophrenia during the resting state. Front Syst Neurosci 5:103.

Zahneisen B, Hugger T, Lee KJ, LeVan P, Reisert M, Lee HL, and others. 2012. Single shot concentric shells trajectories for ultra fast fMRI. Magn Reson Med 68(2):484–94.

Zalesky A, Cocchi L, Fornito A, Murray MM, Bullmore E. 2012. Connectivity differences in brain networks. Neuroimage 60(2):1055–62.

Zeff BW, White BR, Dehghani H, Schlaggar BL, Culver JP. 2007. Retinotopic mapping of adult human visual cortex with high-density diffuse optical tomography. Proc Natl Acad Sci U S A 104(29):12169–74.

Zhang D, Raichle ME. 2010. Disease and the brain's dark energy. Nat Rev Neurol 6(1):15–28.

Zhang H, Duan L, Zhang Y-J, Lu C-M, Liu H, Zhu C-Z. 2011. Test–retest assessment of independent component analysis-derived resting-state functional connectivity based on functional near-infrared spectroscopy. Neuroimage 55(2):607–15.

Zhang H, Zhang Y-J, Lu C-M, Ma S-Y, Zang Y-F, Zhu C-Z. 2010. Functional connectivity as revealed by independent component analysis of resting-state fNIRS measurements. Neuroimage 51(3):1150–61.

Zhang Y-J, Duan L, Zhang H, Biswal BB, Lu C-M, Zhu C-Z. 2012. Determination of dominant frequency of resting-state brain interaction within one functional system. PLoS One 7(12):e51584.

Zhang Y-J, Lu C-M, Biswal BB, Zang Y-F, Peng D-L, Zhu C-Z. 2010. Detecting resting-state functional connectivity in the language system using functional near-infrared spectroscopy. J Biomed Opt 15(4):047003-8.